Eur. Phys. J. B **40**, 421–426 (2004)
DOI: 10.1140/epjb/e2004-00231-9

THE EUROPEAN PHYSICAL JOURNAL B

Characterising and controlling surface defects

E. Carrasco[a], O. Rodríguez de la Fuente, M.A. González, and J.M. Rojo

Departamento de Física de Materiales. Universidad Complutense, 28040 Madrid, Spain

Received 29 January 2004 / Received in final form 16 May 2004
Published online 10 August 2004 –

Abstract. The controlled production of surface defects by ion irradiation and nanoindentation techniques is discussed. The characterisation of novel types of defects is emphasized, among those: quasi two-dimensional dislocation dipoles following coalescence at the surface of the vacancies induced by the irradiation and 'mesas' and 'winding-loops' as dislocation configurations originated by nanoindentation. The relationship between the latter defects and the onset of crystal plasticity is examined.

PACS. 61.72.Ff Direct observation of dislocations and other defects (etch pits, decoration, electron microscopy, X-ray topography, etc.) – 68.35.Gy Mechanical properties; surface strains – 61.72.Bb Theories and models of crystal defects

1 Introduction

The role of crystal defects in the physical properties of crystals has long been recognised. Defects not only influence most of these properties but they actually control some of them, for example mechanical properties or optical properties of insulators. Any standard textbook on Solid State Physics devotes one or more chapters to the study of crystal defects and there are also many books entirely devoted to a specific type of defects such as point defects or dislocations [1]. In the last few years, an ever increasing attention has also been devoted to the subject of Surface Physics, the interest of this science having been certainly nurtured by the surge in the study of nanostructures in which most of the atoms are near a surface. However, these two subjects do not seem to have converged although the potential importance of surface defects has been acknowledged for many years, for example in regard of the increase of chemical reactivity associated therewith [2]. There are no specific textbooks on Surface Defects and the different classifications of scientific subjects do not include an entry with such a name, or an equivalent one. This is possibly linked to the absence, until very recently, of suitable techniques capable of identifying and characterising surface defects at the atomic level, in contrast to well-established techniques, like transmission electron microscopy, which have so much contributed to our present understanding of crystal defects in the bulk. The recent advent of scanning tunnelling microscopy (STM) and related techniques has significantly changed this state of affairs and paved the way to the characterisation of surface defects and to an increasing understanding of their role in the physico-chemical properties of the solids. Crystal defects *in the bulk* can be introduced by a variety of processes: e.g. quenching introduces mainly vacancies, particle irradiation (with electrons, neutrons etc) injects into the lattice both vacancies and interstitials and mechanical deformation introduces chiefly dislocations. One obviously needs similar techniques tuned to the production of surface defects [3]. In the last few years, our group, together with other laboratories, have explored two techniques suitable for the controlled production of surface defects: ion irradiation and nanoindentation. In the present report, we review the main advances achieved, in particular regarding the very specific dislocation configurations originated and their relation to the mechanical properties of the solid. We also report some new calculations, which have allowed us to gain insight into the physics of the dislocation emission around nanoindentations. Most of the experimental results have been obtained by STM whereas simulations based on molecular dynamics approach with suitably defined potentials have been carried out in parallel to provide a sound basis for modelling the different defect structures. Our investigations also show that the standard theory of dislocations in an elastic continuum provides a firm theoretical framework to describe defects configurations near the surface.

2 The production of surface defects

In order to generate surface defects, we have used two types of experimental techniques: ion irradiation and nanoindentation. Both can be controlled in terms of a short number of parameters resulting in a variety of configurations. Some of these defect configurations had not been observed before and their analysis has allowed us to gain further insight in the physics of the interaction processes at surfaces.

[a] e-mail: esther@material.fis.ucm.es

2.1 Ion irradiation

Our bombardment of metallic surfaces is carried out with low energy noble gas ions -energies of the order of 1 keV. When an ion of this type impinges on a surface a number of complicated events take place [4], which are strongly dependent on parameters such as ion fluence or surface temperature. Because of the short range of these ions (only a few interatomic distances), the damage is restricted to a sub-surface region about 1 nm deep. Apart from its interest in regard of the creation of surface defects, low-energy-beam surface modification is also becoming increasingly more important for scientific and technological purposes, from the cleaning of surfaces to the controlled modification of their physical or chemical properties by implantation.

Under the usual conditions of our experiments: Au(001) or Pt(001) metallic surfaces at room temperature, and an Ar^+ ion flux of around 10^{13} ions cm^{-2} at 600 eV of kinetic energy, the evolution of the surface damage as a function of the fluence (total dose) is shown in Figure 1. We use units of θ^+, where $\theta^+ = 1$ implies a fluence of 1 ion per unreconstructed surface atom, equal to 1.20×10^{15} ions cm^{-2} for Au(001). Regarding the sequence (b) to (d), for fluences in the range $0.2 < \theta^+ < 70$ (we obtain the typical sequence of small vacancy islands, coalescence and formation of large vacancy islands ending with the quasi-periodic multi-story arrangement of pits of (d). In fact, the theory predicts [4] a primary damage resulting from low-energy irradiation of metal surfaces, which consists mainly of vacancies in the surface region. If the displacement energy is of the order of 30 eV, the number of atom displacements produced by an incoming ion of 600 eV on Au does not exceed a figure of about 10. As most of the defect pairs produced by these displacements recombine, the total yield of vacancies per collision event is not likely, then, to exceed three. In various earlier experiments on unreconstructed surfaces [5], vacancy islands, such as those shown in Figures 1b and 1c which cannot be associated to single ion collision events, have indeed been observed and have been explained in terms of nucleation and growth following single-vacancy diffusion. However, for the low fluence of Figure 1a, $\theta^+ \approx 0.05$, a novel type of defect is observed. It will be dealt with in the next section.

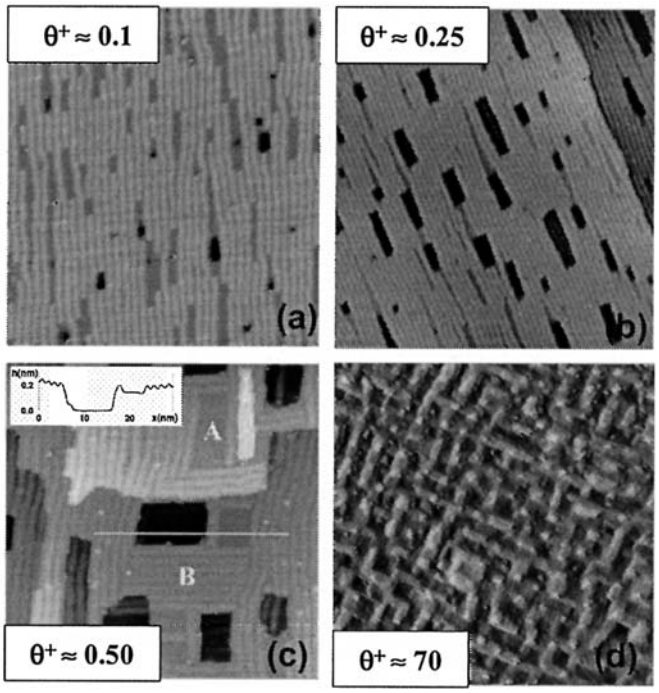

Fig. 1. STM image of a Au(001) surface bombarded with 600 eV Ar^+ ions at room temperature for different fluences: (a) $\theta^+ \approx 0.1$, (55×55 nm^2), (b) $\theta^+ \approx 0.25$ (81×81 nm^2), (c) $\theta^+ \approx 0.5$ (45×45 nm^2), (d) $\theta^+ \approx 70$ (680×680 nm^2). Au(001) is a 5×20 reconstructed surface: the black stripes of the image correspond to the bottom of the ridges in the corrugated-like surface with a periodicity of 1.44 nm.

2.2 Nanoindentation

Microindentation has been used for decades to characterise the mechanical properties of solids and different tests have been devised to actually measure a number of important parameters related to them, chiefly hardness parameters. Going down about three orders of magnitude, nanoindentation is being developed by our group and others as a promising technique to explore the mechanical properties of solid surfaces [6–8]. We are currently using an STM tip (polycristalline W tip) to carry out the nanoindentations. They are performed by letting the tungsten tip progress towards the sample once the tunneling current has been established. This procedure is done manually and with the feedback switched off, pushing the tip gently towards the surface and retracting it, as soon as the tunneling current reaches a saturation value. Once the nanoindentation is done, the feedback is connected again and an image is acquired with the same tip. The image taken just after nanoindentation has enough quality to clearly show the defect structure around the nanoindentation point. This allows us to follow the individual behaviour of a single dislocation (loop) during its creation and further motion. The experiments have been supplemented by atomistic simulations, particularly molecular dynamics computations [9,10].

We can control the size and shape of the nanoindentation traces by changing a short number of parameters such as tip voltage and tunnelling current. Bias voltage permits to adjust the size in such a way that bigger nanoindentations are obtained by decreasing voltage values. An example of the reproducibility of the technique is shown as Figure 2 in which a series of four different nanoindentations have been performed near to each other on a Au(001) surface with a W tip. Notice that the traces sides are parallel to the $\langle 110 \rangle$ compact directions of the Au(001) surface and that the shape of the trace does not seem to depend much on the tip shape, which points out to an efficient diffusion process taking place after the contact.

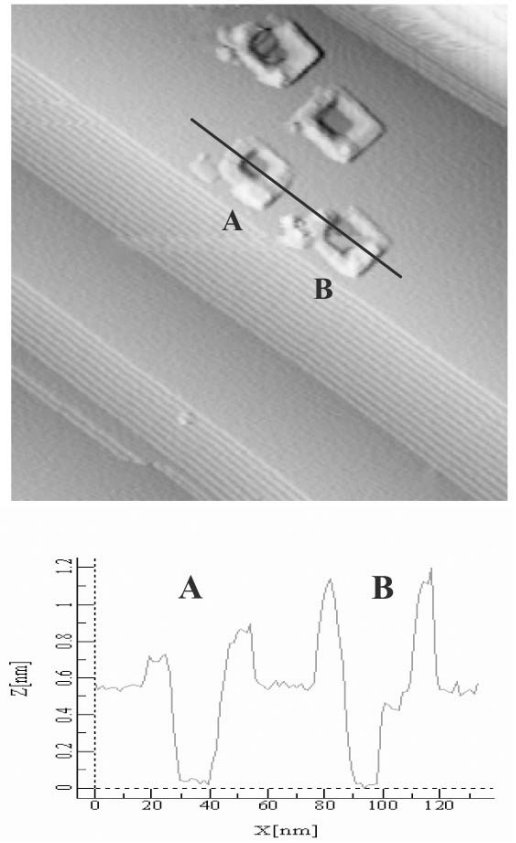

Fig. 2. STM image (270×270 nm^2) of four different nanoindentations performed on a Au(001) surface with a W tip with similar nanoindentations parameters. Note the reproducibility and shallowness of the traces.

3 New types of surface defects

By either ion irradiation or nanoindentation, our experiments have revealed the existence of novel types of surface defects, more specifically, of dislocation configurations. In this section we describe these new defects and propose an interpretation of their structure and origin.

3.1 Two dimensional dislocation dipoles

We have established that the defects shown in Figure 1a are two dimensional (2D) dislocation dipoles. Figure 3a shows a close-up of some of them in an image that also shows some vacancy islands to make it clear that they are not the same defect. These 2D dislocation dipoles are the two-dimensional counterpart of the well-known three-dimensional Frank or Shockley loops created in the bulk of metals following, for example neutron irradiation. As is well-known, the latter result from the collapse of vacancy (or interstitial) discs originated by accretion of the corresponding point defects on compact planes. We propose that our 2D dislocation dipoles arise from a similar mechanism. We have carried out molecular dynamics simulations which show that single vacancies generated all over the surface tend to migrate to the top of the reconstruction ridges and, then, diffuse anisotropically along the reconstruction directions $\langle 110 \rangle$. Although, some of the elementary steps involve complex routes, the kinetic process as a whole leads to vacancy rows on top of the ridges. The simulations also show that they collapse and end up as 2D dislocation dipoles. A dislocation dipole resulting from a simulation is shown in Figure 3b. Note that 2D dislocation dipoles are different from 2D vacancy islands observed at much higher fluences, although the latter have been shown to be nucleated at the dipoles [11]. These 2D dipoles should not either be confused with the several systems of misfit dislocations that have been extensively described in the literature of multilayer growth and which are sometimes called surface dislocations. The defects described in the present paper are perhaps the first direct experimental realisation in a homogeneous system of those 2-D dislocations, which have received much theoretical attention, particularly in connection with order-disorder 2D transitions [12]. The 'floating' nature of the reconstructed overlayer [13] is likely to play a role in the creation of these 2D dislocation structures. It is also worth pointing out that preliminary results indicate that these dipoles show an enhanced chemical reactivity around the emergency points of the corresponding 2D dislocations.

3.2 Mesas

We have discovered [14] a novel complex dislocation configuration which we shall call 'mesa' [15] of which an STM image is shown in Figure 4. As shown, a mesa consists of two pairs of Shockley partial dislocations on contiguous {111} planes, each pair encompassing a stacking-fault. The defect can glide parallel to the surface providing non-diffusional dislocation mechanism for transport of matter away from the nanoindentation point. Mesas have been observed to be created by both nanoindentation and ion irradiation. We have proposed [14] that mesas originate from the splitting into Shockley partials of the two arms of a precursor V-shaped perfect loop of interstitial character and Burgers vector a/2 [110]. In a subsequent stage, mesas can glide away from the indentation trace. Depending on the technique employed, the precursor perfect loop may be punched-off by the nanoindentation, as discussed in the next section, or nucleated from the collapse of a disk of interstitials created by the diffusing interstitials knocked-out by the collision process initiated by the irradiated ions. We have shown in Section 2 that, for all our range of fluences, most of the observed surface damage is of vacancy character. It is not, then, unlikely that the subsurface region becomes enriched in interstitials, either in single or multiple configurations, that after a mild annealing may cluster, collapse and give rise to dislocation loops of interstitial character.

3.3 Winding loops

Dislocations with a screw component can be visualised through the traces of the surface steps left behind in the

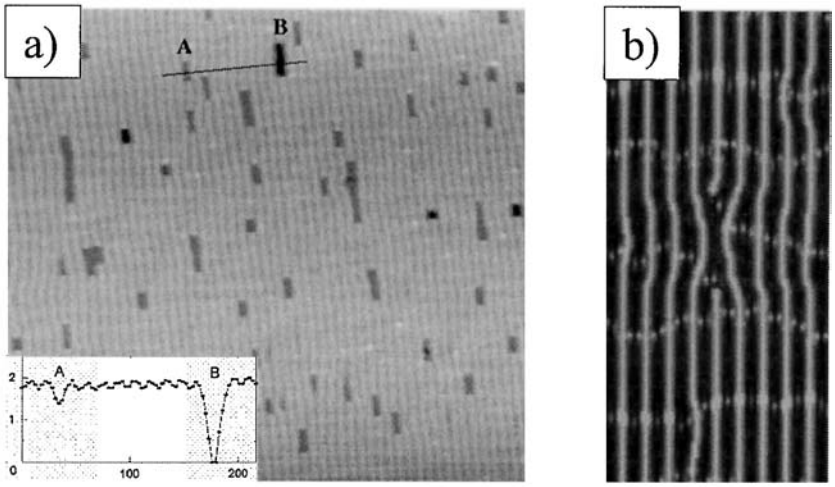

Fig. 3. (a) STM image (50×54 nm^2) of a Au(001) surface bombarded with a fluence of $\theta^+ \approx 0.05$ of 600 eV Ar^+ ions at room temperature. The defects marked A are 2D dislocation dipoles. Compare with surface vacancies, marked B. Inset: Depth profile in Å of both type of defects. (b) Molecular dynamics simulation of a dislocation dipole.

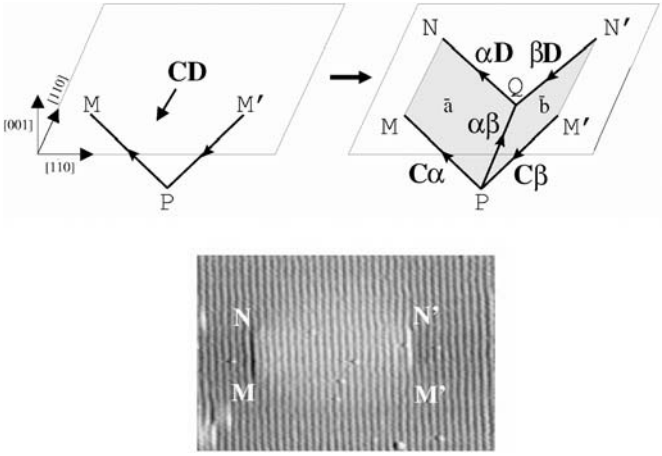

Fig. 4. STM image of a mesa 60×40 nm^2. The dislocation configuration proposed for the defect is the following: An initial loop with Burgers vector **CD** double splits giving rise to four Schockley partial dislocations (α**D**, β**D**, **C**α, **C**β), two stacking faults ($\bar{a}$, $\bar{b}$) and one stair-rod dislocation running along the intersection of the two stacking fault planes. All Burgers vectors in Thompson's tetrahedron notation are shown in the scheme.

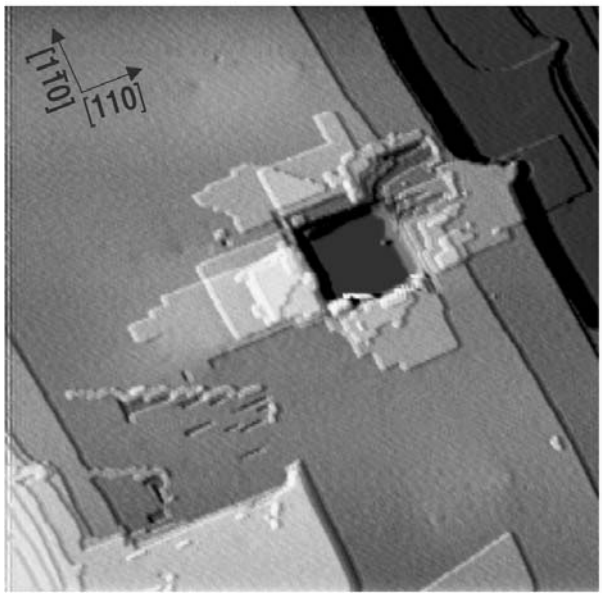

Fig. 5. Terraces around a nanoindentation originated from the cross-slip of dislocation segments with a screw component. 680×680 nm^2 image.

course of their excursions across the surface. We have found [16] that winding terraces one-atomic-step high arise around nanoindentations, as shown in Figure 5. Notice that the trace on the surface of the dislocation motion follows a serrated line, along which changes of gliding direction are clearly visible. Note that all the projected traces of those displacements are at right angles with each other, all the traces being parallel to the $\langle 110 \rangle$ directions in the surface plane. We have interpreted this type of trace in terms of a dislocation segment which cross-slips on adjacent $\{111\}$ planes. A scheme of the mechanism proposed is shown in Figure 6: following nanoindentation, a dislocation loop is created consisting of a segment parallel to the surface and two segments inclined to it. The latter are (at least partially) of a screw character and can glide across the compact (111) planes along the $[1\bar{1}0]$ compact direction, as shown. When the mobile segment cross-slips into the contiguous $(11\bar{1})$ plane, the corresponding surface step sharply bends ninety degrees, as observed in the image. If after a whole turn is completed the segment returns to its original location, one ends up with a closed terrace whereas an (invisible) loop of edge character parallel to the surface is left below. Alternatively, the mobile segment may return to a different point in which case a spiralling terrace is formed. This interpretation of our experiments is supported by molecular dynamics

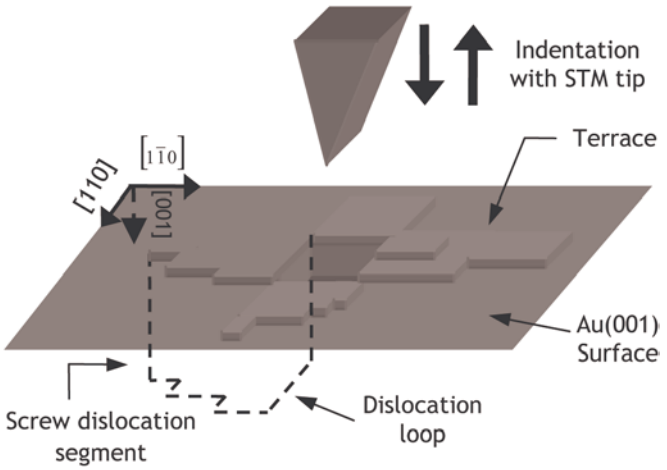

Fig. 6. Scheme showing how a screw segment of a winding loop (generated at a nanoindentation with a STM tip) can give rise to a winding terrace by successive cross-slip. For the sake of simplicity we represent screw dislocation segments perpendicular to the surface, although they lay on {111} planes.

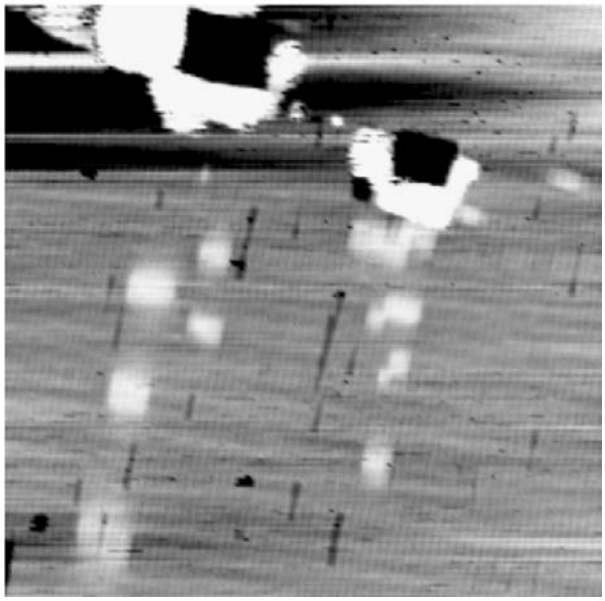

Fig. 7. (98×98 nm^2) STM image of two nanoindentations in the Au(001) surface. Rows of mesas stemming from the nanoindentation points and following a ⟨110⟩ direction are shown.

simulations [17] and calculations based on the elastic theory of dislocations [16].

4 Surface defects and mechanical properties

Although a number of mechanisms of dislocation generation have been proposed [18] – and shown to be operative- it is difficult to account for the rather large number of such dislocations commonly present in any material. At the same time, it has been known for long that the conditions of the surface of solids can strongly influence their mechanical properties [19]. We argue here that surface-sensitive techniques (such as STM), with resolution at the atomic range, can provide new insight into the generation of dislocations at surfaces and into the initial stages of plasticity in solids. We describe now an example of this kind of investigation.

We have reported earlier [8] the emission of rows of mesas along compact directions around the nanoindentation traces, an example of which is shown in Figure 7. Our experimental, together with results from molecular dynamics simulations [8,20], strongly suggest that this emission takes place one dislocation loop at a time. At the same time, other researchers have endeavoured in studying the very first stages of the stress-strain curves in the course of nanoindentations and have proposed that the discontinuous events (in the form of abrupt steps in the curve) that they observe can be traced to the emission of single dislocations, or, at most, of groups involving a few units of them. It is important to note that the emission of a mesa is an individual process, which might well be correlated with the sequence of displacement bursts observed, among others, by Li et al. [21] in their nanoindentation on Al crystals. If this assumption is right, we would be imaging the emission of dislocation loops, at the initial stages of the plastic behaviour of the metal. As a first approximation to a quantitative approach we can assume [11] that the load (force) associated at the tip contact is of the order of 0.01 mN (1 dyn). We, then, take the measured value of the area of the nanoindentation trace (typically around 10^3 nm^2) to obtain an applied stress of 10^{11} dyn cm^{-2}, constant over the area of the trace. The well-known expressions for the spatial distribution of stresses resulting from the application of a point load on a semi-infinite body [22] are easily generalised to the case of a distributed load [23]. With the help of these stresses, the shear forces tending to operate a slip system (111), [1$\bar{1}$0] in a direction parallel to the surface are calculated. The results are shown in Figure 8. Note that the maximum shear force obtained can attain the theoretical critical shear stress, which is of the order of $\mu/2\pi$, being μ the shear modulus. According to the data of Figure 8, dislocation loops with a Burgers vector $\mathbf{b} = (\mathbf{a}/2)$ [110] are generated below the nanoindentation trace and further glide along [110]. Eventually, they are pinned by some kind of barrier (perhaps, impurity related) and result in the spatial distribution of Figure 7. Note that in many cases, instead of a single mesa, a pair of mesas are nucleated, which run parallel to each other. This can also be accounted for by the calculations of Figure 8, as one can see that the maximum shear force – resulting in mesa nucleation – does not peak at $x = 0$ but is practically constant in all the central region of the trace, favouring, then, nucleation of a mesa at any point below the corresponding region of the trace.

5 Conclusions

We have shown that a wide variety of surface defects can be produced now in a controlled way, allowing the characterisation of the mechanisms involved in their generation

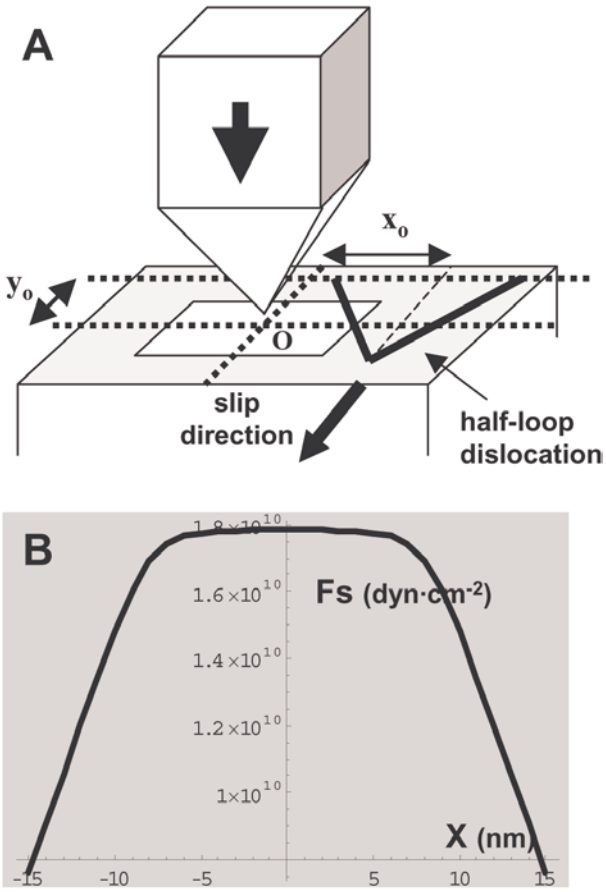

Fig. 8. Calculated shear force Fs across the slip planes and along the slip direction parallel to the surface for a nanoindentation load of 0.01 mN operating uniformly on a 28×28 nm area. A) Scheme explaining location of the half-loop dislocation – V-shaped perfect loop – and its slip direction **y** for graphic B) which shows how the shear force Fs ($\mathrm{dyn\,cm^{-2}}$) varies along direction **x** (nm).

and paving the way for studying the role of surface defects in the different physico-chemical properties of solids. Quasi-two-dimensional surface dislocation dipoles of a vacancy character have been characterised following ion irradiation and preliminary results indicate that these dipoles show an enhanced chemical reactivity. We have also shown that indentation, a powerful technique to study mechanical properties of solids, can be readily extended down to the nanometer scale using the STM tip and that the dislocation configurations introduced by the tip may help elucidating the initial stages of plasticity in solid surfaces.

References

1. F. Agulló-López, C.R.A. Catlow, P.D. Townsend, *Point Defects in Materials* (Academic, London, 1988)
2. There are many suggestions in the literature of the influence of defects on surface reactivity. However, a systematic analysis is still lacking. For a study of the influence of steps, see e.g. T. Zambelli, J. Wintterlin, J. Trost, G. Ertl, Science **273**, 1688 (1996) and for the influence of dislocations see e.g. J. de la Figuera, K. Pohl, A.K. Schmid, N.C. Bartelt, R.Q. Hwang, Surf. Sci. **415**, L993 (1998)
3. When one speaks of *surface defects*, some agreement has to be found concerning the extent of the term 'surface'. Usually, the term is not restricted to the very last plane of atoms in the solid but to the shallow subsurface region (only a few atomic distances deep) in which the atoms feel the asymmetry due to the lack of a half-space
4. M. Nastasi, J.W. Mayer, J.K. Hirvonen, *Ion-Solid Interactions: Fundamentals and Applications* (Cambrige University Press, Cambridge, 1996)
5. Th. Michely, K.H. Besocke, G. Comsa, Surface Sci. Lett. **230**, L135 (1990); C.A. Lang, C.F. Quate, J. Nogami, Appl. Phys. Lett. **59**, 1696 (1991); J.C. Girard, Y. Samson, S. Gauthier, S. Rousset, J. Klein, Surf. Sci. **302**, 73 (1994); M. Esser, K. Morgenstern, G. Rosenfeld, G. Comsa, Surf. Sci. **402**, 341 (1998)
6. U. Landmann, W.D. Luetke, N.A. Burnham, R.J. Colton, Science **248**, 454 (1990)
7. J.D. Kiely, J.E. Houston, Phys. Rev. B **57**, 12588 (1998)
8. O. Rodríguez de la Fuente, J.A. Zimmerman, M.A. González, J. de la Figuera, J.C. Hamilton, W.W. Pai, J.M. Rojo, Phys. Rev. Lett. **88**, 036101 (2002)
9. C.L. Kelchner, S.J. Plimpton, J.C. Hamilton, Phys. Rev. B **58**, 11085 (1998); J.A. Zimmerman, C.L. Kelchner, P.A. Klein, J.C. Hamilton, S.M. Foiles, Phys. Rev. Lett. **87**, 165507 (2001)
10. A. Gannepalli, S.K. Mallapagrada, Phys. Rev. B **66**, 104103 (2002)
11. O. Rodríguez de la Fuente, M.A. González, J.M. Rojo, Phys. Rev. B **63**, 085420 (2001)
12. D.R. Nelson, in *Phase Transitions*, Vol. 7 (Academic Press, London, 1983), pp. 1–99. For recent calculations with a *glue* potential see F. Celestini, F. Ercolessi, E. Tosatti, Phys. Rev. Lett. **76**, 3153 (1999)
13. V. Fiorentini, M. Methfessel, M. Scheffler, Phys. Rev. Lett. **71**, 1051 (1993)
14. J. de la Figuera, M.A. González, R. García-Martínez, J.M. Rojo, O.S. Hernán, A.L. Vázquez de Parga, R. Miranda, Phys. Rev. B **58**, 1169-72 (1998)
15. 'Mesa' seems a more proper name than the initially coined of 'hillock' because the height of the configuration, 0.6 Å, is very small compared compared to the defect trace of the order of a few nanometers
16. E. Carrasco, O. Rodríguez de la Fuente, M.A. González, J.M. Rojo, Phys. Rev. B (Rapid Communications) **68**, 108102(R) (2003)
17. Krystyn J. Van Vliet, Ju Li, Ting Zhu, Sidney Yip, Subra Suresh, Phys. Rev. B **67**, 104105 (2003) and Ju Li, `http://www.mse.eng.ohio-state.edu/fac-staff/faculty/li/candidate_b2.html`
18. See e.g. J.P. Hirth, J. Lothe, *Theory of Dislocations*, 2nd edn. (McGraw-Hill, New York, 1972), pp. 682–693
19. S.J. Basinski, Z.S. Basinski, *Plastic Deformation and Work Hardening* in *Dislocations in Solids*, Vol. 4, edited by F.R.N. Nabarro (North-Holland Publishing Company, Amsterdam, 1979), pp. 261–362
20. J. de la Figuera, private communication
21. J. Li, K.J. Van Vliet, T. Zhu, S. Yip, S. Suresh, Nature (London) **418**, 307 (2002)
22. L.D. Landau, E.M. Lifshitz, *Theory of Elasticity* (Pergamon, New York, 1959), p. 29
23. A.E.H. Love, *A Treatise on the Mathematical Theory of Elasticity* (Dover, New York, 1944), p. 191